Control in effort of a robotic hand

2017 / 2018

Veronica Elena

20/03/2018

State-space representation and observability check

Notations

List of Abbreviation

COM	Centre of mass
DM	Dynamic Model
DoF	Degrees of Freedom

List of symbols

L_i	Length of the i-th phalanx
s_i	Distance between the COM of the i-th phalanx and the next joint
m_i	Mass of the i-th phalanx
I_i	Momentum of inertia of the i-th phalanx
r	Pulley radii
r_m	Radius of the motor shaft
b_i	Thickness of the i-th spring
K_i	Constant of the i-th spring
l	Spring length after a load is applied
l_0	Spring length in rest position
$\mathbf{\Gamma}$	Input torque vector
$\mathbf{\Gamma_f}$	Input torque vector given by friction effect
$\mathbf{\Gamma_e}$	Input torque vector given by external forces
$\mathbf{F}$	Vector of external forces
$\mathbf{J}$	Jacobian matrix
L	Lagrangian
E	Kinetic Energy
U	Potential Energy
$\mathbf{q}$	Joint coordinates vector
$\dot{\mathbf{q}}$	Joint velocities vector
$\ddot{\mathbf{q}}$	Joint acceleration vector
$\mathbf{q_m}$	Motor coordinates vector
$\mathbf{v}$	Velocity of the fingertip
$\mathbf{A}$	Inertia matrix
$\mathbf{C}$	Matrix of Coriolis and centrifugal effects
$\mathbf{Q}$	Matrix of gravitational effect
$\mathbf{F_v}$	Matrix of Coulomb parameters
$\mathbf{f_s}$	Vector of viscous friction parameters
I_{aj}	Equivalent inertia of the joint velocity
N_j	Transmission ratio of the joint j axis
J_{mj}	Moment of inertia of the rotor and transmission of actuator j
Σ	Control system
$\mathbf{x}$	State vector
$\mathbf{u}$	Input vector
$\mathbf{y}$	Output vector
$f(\cdot)$	Meromorphic function
$h(\cdot)$	Meromorphic function
X	State space
U	Input space
Y	Output space
O	Observability filtration
O_∞	Observable space of the system Σ
$\mathbf{L}$	Observability matrix

Chapter 1

Alpes Instruments robotic hand

1.1 Design presentation

Alpes Instruments, a French company that studies and designs mechanical and electronic products in stringent environments, designs an anthropomorphic robotic hand with 15 DoF and 6 actuators. Since the number of DoF is bigger than the number of actuators, it is classified an underactuated hand. The hand is inspired to a human hand, indeed it has similar size, weight (0.62 kg) and aspect. It is composed of four fingers with three phalanges each one and a thumb with only two phalanges (Figure 1.1).
Each finger is equipped with a 12 V DC electric motor which has a current sensor and an encoder. The torque is transmitted to the passive joints via a system of pulleys and cables.

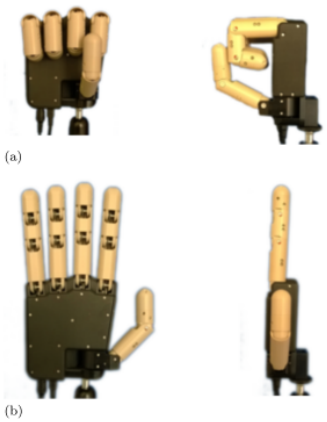

Figure 1.1: (a) CAD model of the hand in a flexed position and (b) in an extended position[1]

The thumb has two electric motors. The first controls the adduction and abduction movements, while the second controls the flection and extension movements. The return extension movement is provided by springs placed on each joint.
Considering the geometric model, each finger has tree parallel revolute joints and the thumb also has an additional joint which allows adduction/abduction movements. Each finger has at least one independent motor, thus they can be modelled and controlled independently. The hand is modelled as a tree-structure with the origin of the reference frame which is located in the middle of the palm.

1.2 Physical parameters

Table (1.2) contains the physical parameters values of the *Alpes Instruments* robotic hand. The lengths, the masses and the pulley radii of each phalanx values are provided by the company itself. Other parameters as the distance of the centre of mass of the i-th phalanx from the next joint (s), the moment of inertia and the springs parameters have been measured or estimated. In particular, the COM position of each link is assumed in the centre of each phalanx, thus:

$$s_i = \frac{L_i}{2}, \qquad i = 1, 2, 3.$$

Concerning the momentum of inertia, each phalanx has been modelled as a rod rotating around its end: the rotation axis corresponds to the joint axis. Using this model the parameter is computed as follows:

$$I_i = \frac{1}{3} m_i L_i^2, \qquad i = 1, 2, 3.$$

Finally, each spring is characterized by a thickness (b) and a spring constant (K). Concerning the first parameter, it is assumed that all springs has the same thickness and it is set to 0.003 [m]. The spring constant values increase coming towards the fingertip and they are 0.04, 0.05 and 0.06 $[\frac{Nm}{rad}]$ respectively. However, these parameters will be better estimated later on.

Parameter	Value	Unit	Description
L_1	0.05	m	length of the first phalanx
L_2	0.03	m	length of the second phalanx
L_3	0.024	m	length of the third phalanx
s_1	0.025	m	distance between next joint and considered phalanx's COM
s_2	0.015	m	distance between next joint and considered phalanx's COM
s_3	0.012	m	distance between next joint and considered phalanx's COM
m_1	0.03	kg	mass of the first phalanx
m_2	0.02	kg	mass of the second phalanx
m_3	0.023	kg	mass of the third phalanx
I_1	2.5000e-05	$kg \cdot m^2$	momentum of inertia of the first phalanx
I_2	6.0000e-06	$kg \cdot m^2$	momentum of inertia of the second phalanx
I_3	4.4160e-06	$kg \cdot m^2$	momentum of inertia of the third phalanx
r	0.004	m	pulley radii of the phalanges
K_1	0.04	Nm/rad	spring constant on the first phalanx
K_2	0.05	Nm/rad	spring constant on the second phalanx
K_3	0.06	Nm/rad	spring constant on the third phalanx
b	0.003	m	spring thickness

Figure 1.2: Numerical values of the physical parameters used for each finger.

Chapter 2

Dynamic model

2.1 Theoretical material

In [2], the dynamic model of a complex robot is modelled. There exist two main methods to solve this problem: Newton-Euler method and the Lagrangian one. The former is computationally more efficient than the latter one, but the Lagrangian approach is analytically easier. For this reason this last method is used in the following.
The Lagrange formulation describes the behaviour of a dynamic system in terms of work and energy stored in the system. Considering an ideal system without friction or elasticity, exerting neither forces nor moments on the environment, the Lagrange equations are commonly written in the form:

$$\mathbf{\Gamma_i} = \frac{\mathrm{d}}{\mathrm{d}t}\left(\frac{\partial L}{\partial \dot{q}_i}\right)^T - \left(\frac{\partial L}{\partial q_i}\right)^T, \tag{2.1}$$

where Γ is the motor torque, L is the Lagrangian of the robot defined as the difference between the kinetic energy E and the potential energy U of the system (Equation 2.2).

$$\mathbf{L} = \mathbf{E} - \mathbf{U}. \tag{2.2}$$

The kinetic energy of the system is a quadratic function in the joint velocities such that:

$$E = \frac{1}{2}\dot{\mathbf{q}}^{\mathbf{T}}\mathbf{A}\dot{\mathbf{q}}, \tag{2.3}$$

where A is the (nxn) symmetric and positive definite inertia matrix of the robot. Its elements are functions of the joint positions. The (i, j) element of A is denoted by A_{ij}.
Since the potential energy is a function of the joint positions, the equation 2.1 lead to:

$$\Gamma_i = \mathbf{A}(\mathbf{q})\ddot{\mathbf{q}} + \mathbf{C}(\mathbf{q}, \dot{\mathbf{q}})\dot{\mathbf{q}} + \mathbf{Q}(\mathbf{q}), \tag{2.4}$$

where $C(q, \dot{q})\dot{q}$ is the (nx1) vector of Coriolis and centrifugal torques, such that:

$$\mathbf{C}\dot{\mathbf{q}} = \dot{\mathbf{A}}\dot{\mathbf{q}} - \frac{\partial E}{\partial \dot{q}} \tag{2.5}$$

and $\mathbf{Q} = [Q_1....Q_n]^T$ is the vector of gravity torques, $Q_i = \frac{\partial U}{\partial \dot{q}_i}$.

2.1.1 Considering friction

Friction plays a dominant role in limiting the quality of robot performance. Non- compensated friction produces static error, delay, and limit cycle behaviour. Lots of friction models have

been proposed, but the main one is the Coulomb-Viscous friction model. Therefore, the friction torque at i-th joint is written as:

$$\Gamma_{fi} = F_{si}\text{sign}(\dot{q}_i) + F_{vi}\dot{q}_i. \tag{2.6}$$

To take into account the friction in the dynamic model of a robot, we add the vector Γ_f on the right side of equation (2.4) such that:

$$\mathbf{\Gamma_f} = \mathbf{F_v}\dot{\mathbf{q}} + \mathbf{f_s}, \tag{2.7}$$

where $\mathbf{F_v} = \text{diag}([f_{v1}...f_{vn}])$ and $\mathbf{f_s} = [f_{s1}\text{sign}(\dot{q}_1)...f_{sn}\text{sign}(\dot{q}_n)]^T$ indicate the Coulomb and the viscous friction parameters respectively.
The model based on Coulomb friction assumes a constant friction component that is independent of the magnitude of the velocity. The viscous friction is generally represented as being proportional to the velocity. The most often employed model is composed of Coulomb friction together with viscous friction.

2.1.2 Considering the rotor inertia of actuators

The kinetic energy of the rotor (and transmission system) of actuator j, is given by the expression $\frac{1}{2}l_{aj}\dot{q}_j^2$. The inertial parameter l_{aj} denotes the equivalent inertia referred to the joint velocity. It is given by:

$$l_{aj} = N_j^2 J_{mj} \tag{2.8}$$

where J_{mj} is the moment of inertia of the rotor and transmissions of actuator j, N_j is the transmission ratio of joint j axis, equal to $\frac{\dot{q}_{mj}}{\dot{q}_j}$ where $\dot{q}_{mj}$ denotes the rotor velocity of actuator j . In the case of a prismatic joint, l_{aj} is an equivalent mass.
In order to consider the rotor inertia in die dynamic model of the robot, we add the inertia (or mass) l_{aj} to the A_{jj} element of the matrix $\mathbf{A}$.

2.1.3 Considering the forces and moments exerted by the end-effector on the environment

Considering the joint torque vector $\mathbf{\Gamma_e}$ necessary to exert a given wrench $\mathbf{F}$ on the environment is obtained using the basic static equation:

$$\mathbf{\Gamma_e} = \mathbf{J^T F}, \tag{2.9}$$

where $\mathbf{J}$ is the Jacobian matrix of the robotic finger.
Thus, we have to add the vector $\mathbf{\Gamma_e}$ on the right side of equation (2.4).

2.2 Dynamic model of one finger

From the previous section comes out that the complete dynamic model for a rigid robot is:

$$\mathbf{A(q)\ddot{q} + Ia\ddot{q} + C(q,\dot{q})\dot{q} + F_v\dot{q} + f_s + G(q) = \Gamma + J^T F} \tag{2.10}$$

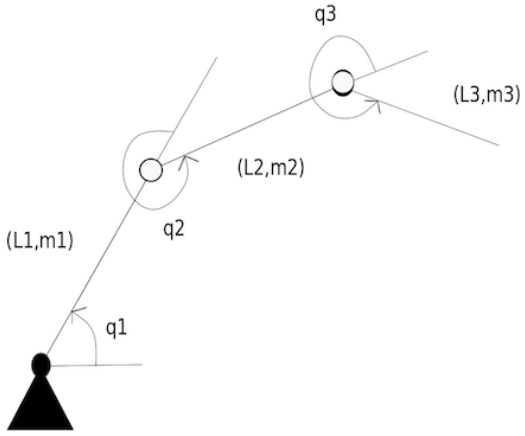

Figure 2.1: Model of the *Alpes Instruments* robotic hand's finger.

Considering the system representing one finger of the *Alpes Instruments* robotic hand (Figure 2.1), the following dynamic model is kept into account:

$$\mathbf{A(q)\ddot{q} + C(q,\dot{q})\dot{q} + G(q) = \Gamma + J^T F} \tag{2.11}$$

where $\mathbf{A(q)}$ is the inertial matrix, $\mathbf{C(q,\dot{q})}$ is the matrix related to the Coriolis and centrifugal forces, $\mathbf{G(q)}$ is a 3x1 vector which represents the gravitational effect and the springs contribution, $\mathbf{\Gamma}$ is the vector representing the motor torque, $\mathbf{J}$ is the Jacobian matrix and $\mathbf{F}$ represents the measured contact forces.
In particular, the Jacobian matrix has the form:

$$\mathbf{J} = \begin{bmatrix} -L_1\sin(q_1) - L_2\sin(q_1+q_2) - L_3\sin(q_1+q_2+q_3) & -L_2\sin(q_1+q_2) - L_3\sin(q_1+q_2+q_3) & -L_3\sin(q_1+q_2+q_3) \\ 0 & 0 & 0 \\ L_1\cos(q_1) + L_2\cos(q_1+q_2) + L_3\cos(q_1+q_2+q_3) & L_2\cos(q_1+q_2) + L_3\cos(q_1+q_2+q_3) & L_3\cos(q_1+q_2+q_3) \end{bmatrix},$$

where L_i are the lengths of the links and q_i are the relative joint coordinates with i = 1,2,3. The Jacobian matrix relates the fingertip velocity ($\mathbf{v}$) to the velocities of the joint coordinates as:

$$\mathbf{\dot{v} = J\dot{q}}. \tag{2.12}$$

Equation (2.11) does not keep into account neither the friction nor the rotor inertia contributions. These terms are neglected in this first phase of investigation in order to consider a simplified system. Their role will be studied afterwards.

The finger is equipped with one FlexiForce sensor which is a force sensing resistor (FSR) sensor. It is able to measure only the normal component of the contact force. Considering the system of reference in (Figure 2.2), it is reasonable to set the force component along the x axis to zero, since the system acts on the yz plane. Moreover it is assumed that also the component along the y axis is zero because the no sliding case is kept into account. Thus, the external force vector has the form:

$$\mathbf{F} = \begin{bmatrix} 0 & 0 & F_z \end{bmatrix}^T. \tag{2.13}$$

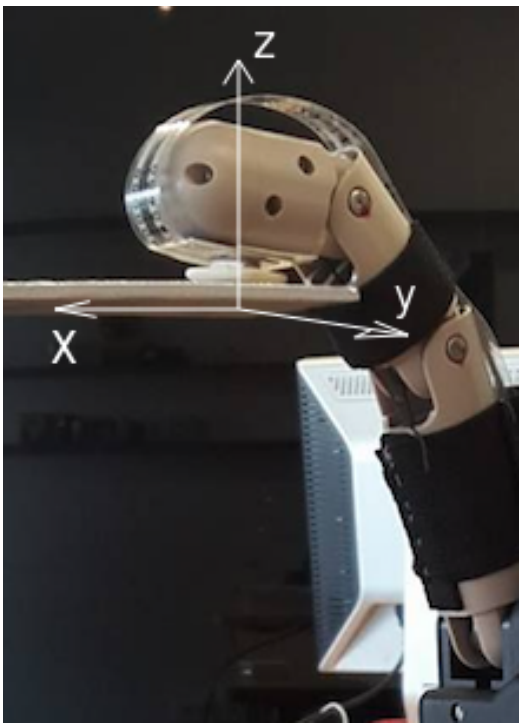

Figure 2.2: Reference frame of the system.

Concerning the potential energy acting on the system, it is composed of the gravitational effect acting along the z axis and the contribution given by the springs. They are place in correspondence of each joint and they enclose around the pulleys when the finger flexes. They are characterized by a thickness (b) and a constant (K). The potential energy of the spring is, by definition, $U_s = \frac{1}{2}K(l - l_0)^2$, where l_0 is the initial length of the spring and l is the length after the load is applied. U_s of the i-th spring can be expressed as function of the corresponding joint coordinate as:

$$U_s = \frac{1}{2}K_i(q_i(\frac{b_i}{2} + r_i))^2. \tag{2.14}$$

This expression comes from geometrical consideration.

Chapter 3

State-space representation

In the previous chapter, the physical characteristics of the robotic hand have been presented. Since each finger is provided by only one actuator and the other joints are driven through a system of pulleys and cables, the joint coordinate variables ($q_i, i = 1, 2, 3$) are not measurable. Moreover, the motor's encoder measures the angular position of the motor (q_m), but it does not coincide with the fist joint variable.
Considering the transmission mechanism, a geometrical relation between q_m and q_i can be found:

$$q_m = \frac{r}{r_m}(q_1 + q_2 + q_3),$$

where r is the pulley radius and r_m is the radius of the motor shaft.
Thus, considering only one finger, it comes out that the output of the system depends on the sum of the joint coordinates.
From this fact it arises the necessity of observing the q_i from the system using an observer. However, the state-space representation of the system has to be defined and then the observability check should be performed before designing the observer.
In the following this topic is faced.

3.1 State-space representation

In the context of control theory, a dynamic system can be represent via its *state-space representation* of the general form [3]:

$$\Sigma = \begin{cases} \dot{x}(t) &= f(x(t), u(t)) \\ y(t) &= h(x(t)) \end{cases} \tag{3.1}$$

In this system, $t \in \mathbb{R}$ denotes time; the state $x(\cdot) \in \mathbb{R}^n$; the input $u(\cdot) \in \mathbb{R}^m$; the output $y(\cdot) \in \mathbb{R}^p$; and the entries of f, h are meromorphic functions.
Considering the control variable:

$$\mathbf{x} = \begin{cases} \mathbf{x_1} = \mathbf{q} \\ \mathbf{x_2} = \dot{\mathbf{q}} \end{cases} \tag{3.2}$$

and $\mathbf{u} = \mathbf{\Gamma}$, equation (3.1) becomes:

$$\begin{cases} \dot{\mathbf{x}}_\mathbf{1} &= \mathbf{x_2} \\ \dot{\mathbf{x}}_\mathbf{2} &= \mathbf{A}(\mathbf{x_1})^{-1}[\mathbf{\Gamma} + \mathbf{J^T}(\mathbf{x_1})\mathbf{F} - \mathbf{C}(\mathbf{x_1}, \mathbf{x_2})\mathbf{x_2} - \mathbf{G}(\mathbf{x_1})] \\ y &= \begin{bmatrix} 1 & 1 & 1 & 0 & 0 & 0 \end{bmatrix} \mathbf{x} \end{cases} \tag{3.3}$$

3.2 Observability

The notion of the observability of a linear or nonlinear dynamic system concerns the possibility of recovering the state $x(t)$ from knowledge of the measured output y(t), the input u(t), and, possibly, a finite number of their time derivatives $y(k)(t), k \geq 0$, and $u(l)(t), l \geq 0$. The structural property which can be easily characterized in a nonlinear framework concerns the existence of an open and dense submanifold of the state space $\mathbb{R}^n$ around whose points the system is locally observable. In order to study the observability property, the system (3.1) will be considered.
Given a system Σ, let us denote by X, U, and Y the spaces defined, respectively, by $X = \text{span}(dx)$, $U = \text{span}(du(j)), j \geq 0$, and $Y = \bigcup_{i \geq 0} Y_i$, where $Y_i = \text{span}(dy(j)), 0 \leq j \leq i$. The chain of subspaces:

$$0 \subset O_0 \subset O_1 \subset O_2 \subset ... \subset O_k \subset ... \tag{3.4}$$

where $O_k := X \cap (Y_k + U)$ is called the observability filtration.
Denoting by O_∞ the limit of the observability filtration, it is easy to see that:

$$O_\infty := X \cap (Y + U). \tag{3.5}$$

Theorem 1 The observable subspace O_∞ of Σ is such that:

$$\dim O_\infty = \text{rank} \left[\frac{\partial(y, \dot{y}, \ddot{y}, ..., y^{n-1})}{\partial x} \right]. \tag{3.6}$$

Theorem 2 A system Σ of the form (3.1) is observable if and only if:

$$O_\infty = X. \tag{3.7}$$

From these theorems, the Observability Criterion follows:

Σ is observable if and only if

$$\text{rank} \left[\frac{\partial(y, \dot{y}, \ddot{y}, ..., y^{n-1})}{\partial x} \right] = n, \tag{3.8}$$

where n is the dimension of the state space.

3.3 Observability check

In this section, the observability properties of the robotic hand system is studied. In particular, in order to apply the *Observability Criterion*, the matrix composed of the partial derivatives of the output with respect to the state vector is build and its rank is analysed.
In the following two systems are investigated: a Two-phalanx system and a Three-phalanx one. The former is a simplification of the real system, while the latter is the complete one. In the case the the system with only two links results unobservable, even the more complex system would be unobservable.

3.3.1 Two-phalanx finger

In order to simplify the analysis of the system observability properties, the system is reduced to a two-phalanx finger (Figure 3.1). Moreover, the friction contribution and the rotor inertia of the actuator are neglected. Considering these simplification, the dynamic model becomes:

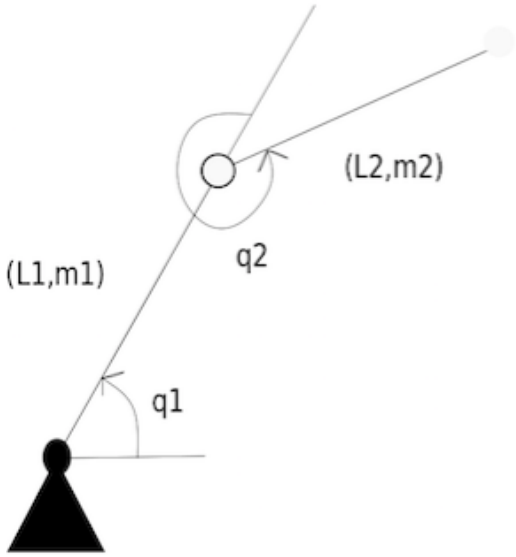

Figure 3.1: Simplified model of the *Alpes Instruments* robotic hand's finger.

$$\mathbf{A}(\mathbf{q})\ddot{\mathbf{q}} + \mathbf{C}(\mathbf{q}, \dot{\mathbf{q}}) + \mathbf{G}(\mathbf{q}) = \mathbf{\Gamma}. \tag{3.9}$$

The control variable are chosen as:

$$\mathbf{x} = \begin{cases} x_1 = q_1 \\ x_2 = q_2 \\ x_3 = \dot{q}_1 \\ x_4 = \dot{q}_2 \end{cases} \tag{3.10}$$

and the corresponding state-space representation becomes:

$$\Sigma = \begin{cases} \dot{x}_1 &= & x_3 \\ \dot{x}_2 &= & x_4 \\ \dot{x}_3 &= & \Phi_1(\mathbf{x}, \mathbf{u}) \\ \dot{x}_4 &= & \Phi_2(\mathbf{x}, \mathbf{u}) \end{cases} \tag{3.11}$$

The functions Φ_i depend on the inverse dynamic model:

$$\begin{bmatrix} \Phi_1 \\ \Phi_2 \end{bmatrix} = \mathbf{A^{-1}}(\mathbf{x_1}, \mathbf{x_2}) \left(\mathbf{\Gamma} + \mathbf{J^T}(\mathbf{x_1}, \mathbf{x_2})\mathbf{F} - \mathbf{C}(\mathbf{x_1}, \mathbf{x_2}, \mathbf{x_3}, \mathbf{x_4}) \begin{bmatrix} \mathbf{x_3} \\ \mathbf{x_4} \end{bmatrix} - \mathbf{G}(\mathbf{x_1}, \mathbf{x_2}) \right). \tag{3.12}$$

A similar model has been studied in [4].

As said before, since only the first joint is actuated, each finger has only one encoder. It returns the angular position of the motor (q_m), thus the value of the first joint coordinate is not directly available. Moreover, the second joint is driven by a system of pulleys and cables and the joint coordinate values are not easily accessible. The following relation between the encoder measurement and the joint coordinates is valid:

$$q_m = \frac{r}{r_m}(q_1 + q_2). \tag{3.13}$$

For these reasons, the output of the state-space representation is considered as to the sum of the joint coordinates $y = x_1 + x_2$.
The input of the system is the motor toque $\mathbf{u} = \mathbf{\Gamma}$.
The corresponding Observability matrix has the following expression:

$$\mathbf{L} = \begin{bmatrix} \frac{\partial y}{\partial \mathbf{x}} & \frac{\partial \dot{y}}{\partial \mathbf{x}} & \frac{\partial \ddot{y}}{\partial \mathbf{x}} & \frac{\partial y^{(3)}}{\partial \mathbf{x}} \end{bmatrix}^T. \tag{3.14}$$

In this system the dimension of the state space X is $n = 4$. From the previous discussion it comes out that the considered system is observable if and only if $\text{rank}(L) = n = 4$.
A Matlab code has been implemented in order to check the observability property of the above presented system. It results that the system is observable.

3.3.2 Three-phalanx finger

Since the simplified system composed of only two phalanges results observable, the study is enlarged to the complete system (Figure 2.1). The above mentioned discussion is still valid, but the control variables become:

$$\mathbf{x} = \begin{cases} x_1 = q_1 \\ x_2 = q_2 \\ x_3 = q_3 \\ x_4 = \dot{q}_1 \\ x_5 = \dot{q}_2 \\ x_6 = \dot{q}_3 \end{cases} \tag{3.15}$$

and the corresponding state-space representation becomes:

$$\Sigma = \begin{cases} \dot{x}_1 = x_4 \\ \dot{x}_2 = x_5 \\ \dot{x}_3 = x_6 \\ \dot{x}_4 = \Phi_1(\mathbf{x}, \mathbf{u}) \\ \dot{x}_5 = \Phi_2(\mathbf{x}, \mathbf{u}) \\ \dot{x}_6 = \Phi_3(\mathbf{x}, \mathbf{u}) \end{cases} \tag{3.16}$$

In this second case of study, the dimension of the state space is n = 6 and the output is the sum of the three joint coordinates:

$$y = x_1 + x_2 + x_3.$$

Also in this case $\mathbf{u} = \mathbf{\Gamma}$.
Computing the observability matrix L, defined in (3.14), via the corresponding Matlab code and applying the observability criterion, the system results still observable.
Thank to this result, the necessary condition for designing an observer is satisfied and different techniques of synthesis can be investigated.

Conclusion

When the state is not directly measurable but its value is required for computing a feedback, the use of an observer is important. In contrast to the linear situation, observability of a given nonlinear system is necessary but not sufficient to assure the possibility of constructing an observer [3].
The aim of this report is to present the observability properties of a underactuated robotic finger with three DoF and only one actuators. The passive joints are driven via a system of pulleys and cable, and one spring on each joint is placed in order to ensure the return to the rest position where the finger is completely stretched.
The system is dynamically studied [2] neglecting the friction and rotor inertia effects and the state-space representation is modelled [3]. Finally, the observability of the system is analysed using the Observability Criterion (Equation 3.8).
From the above discussion results that the considered system is observable, thus it is possible to investigate the synthesis of an observer.

Bibliography

[1] E. Matheson, Y. Aoustin, E. Le Carpentier, A. Leon, and J. Perrin, "Anthropomorphic underactuated hand with 15 joints," in *New Trends in Medical and Service Robots*. Springer, 2016, pp. 277–295.

[2] W. Khalil, E. Dombre, J.-P. Merlet, F. Pierrot, P. Wenger, M. Haddad, T. Chettibi, H. Lehtihet, P. Dauchez, P. Fraisse *et al.*, *Modeling, performance analysis and control of robot manipulators*. Wiley Online Library, 2007.

[3] G. Conte, C. H. Moog, and A. M. Perdon, *Algebraic methods for nonlinear control systems*. Springer Science & Business Media, 2007.

[4] B. Cherki, Y. Aoustin, and P. Lemoine, "An experimental validation of a nonlinear velocities observer," *IFAC Proceedings Volumes*, vol. 28, no. 8, pp. 355–359, 1995.